https://doi.org/10.5194/soil-2019-88
Preprint. Discussion started: 4 December 2019

SOIL Discussions Open Access EGU

Boreal forest soil chemistry drives soil organic carbon bioreactivity along a 314-year fire chronosequence

Benjamin Andrieux[1], David Paré[2], Julien Beguin[2], Pierre Grondin[3], Yves Bergeron[1]

[1]NSERC-UQAT-UQAM Industrial Chair in Sustainable Forest Management, Forest Research Institute, Université du Québec en Abitibi-Témiscamingue, Rouyn-Noranda, QC, J9X5E4, Canada
[2]Natural Resources Canada, Canadian Forest Service, Laurentian Forestry Centre, Québec, QC, G1V4C7, Canada
[3]Ministère des Forêts, de la Faune et des Parcs, Direction de la Recherche Forestière, Québec, G1P3W8, Canada

Correspondence to: Benjamin Andrieux (benjamin.andrieux@uqat.ca)

Abstract. Following wildfire, organic carbon (C) accumulates in boreal forest soils. The long-term patterns of accumulation as well as the mechanisms responsible for continuous soil C stabilization or sequestration are poorly known. We evaluated post-fire C stock changes in functional reservoirs (bioreactive and recalcitrant) using the proportion of C mineralized in CO_2 by microbes in a long-term lab incubation, as well as the proportion of C resistant to acid hydrolysis. We found that all soil C pools increased linearly with time since fire. The bioreactive and acid-insoluble soil C pools increased at a rate of 0.02 $MgC.ha^{-1}.yr^{-1}$ and 0.12 $MgC.ha^{-1}.yr^{-1}$, respectively, and their proportions relative to total soil C stock remained constant with time since fire (8% and 46%, respectively). We quantified direct and indirect causal relationships among variables and carbon bioreactivity to disentangle the relative contribution of climate, moss dominance, soil particle size distribution and soil chemical properties (pH, exchangeable Mn and Al, and metal oxides) to the variation structure of *in vitro* soil carbon bioreactivity. Our analyses showed that the chemical properties of Podzolic soils that characterise the study area were the best predictors of soil carbon bioreactivity. For the FH horizon (O-layer), pH and exchangeable Mn were the most important (model-averaged estimator for both: 0.34) factors directly related to soil organic C bioreactivity, followed by time since fire (0.24), moss dominance (0.08) and climate and texture (0 for both). For the mineral soil, exchangeable aluminum was the most important factor (model-averaged estimator: -0.32), followed by metal oxide (-0.27), pH (-0.25), time since fire (0.05), climate and texture (~ 0 for both). Of the four climate factors examined in this study (i.e., mean annual temperature, growing degree-days above 5°C, mean annual precipitation and water balance) only those related to water availability, and not to temperature, had indirect effect (FH horizon) or a marginal indirect effect (mineral soil) on soil carbon bioreactivity. Given that predictions of the impact of climate change on soil carbon balance are strongly linked to the size and the bioreactivity of soil C pools, our study stresses the need to include the direct effects of soil chemistry and the indirect effects of climate and soil texture on soil C decomposition in Earth System Models to forecast the response of boreal soils to global warming.

1 Introduction

Soil is the largest terrestrial carbon (C) reservoir (Scharlemann et al., 2014) and a major source of uncertainty in ecosystem C predictions (Shaw et al., 2014). Therefore, an advanced mechanistic understanding of soil C processes needs to be investigated and integrated into forecast models to reduce uncertainties in global carbon-cycle feedback projections and to better predict the effects of global change on soil C reservoir (Bradford et al., 2016; Schmidt et al., 2011). The maintenance of the vast soil C reservoir is partly under microbial control (Cotrufo et al., 2013) and could respond to variations in environmental conditions (Davidson and Janssens, 2006). Hence, the carbon-quality temperature hypothesis states that more "recalcitrant" soil organic matter should have higher temperature sensitivity (Craine et al., 2010; Fierer et al., 2005). According to this hypothesis, it is important to distinguish the recalcitrant portion of the soil organic matter from the active portion in order to predict the impact of a rise in temperature on soil heterotrophic respiration.

https://doi.org/10.5194/soil-2019-88
Preprint. Discussion started: 4 December 2019

Wildfire is a major natural disturbance in boreal forests that drives the ecosystem carbon balance (Bond-Lamberty et al., 2007; Kurz et al., 2013) and is known to impact several soil properties, including organic matter quantity and quality (Certini, 2005; Knicker, 2007). Key soil properties, some evolving following fire (e.g., soil acidity) and some not (e.g., particle size distribution), interact with climate and vegetation composition in complex causal direct and indirect relationships to regulate post-fire soil C accumulation (Andrieux et al., 2018). A saturation of soil C accumulation, especially for its recalcitrant portion, is often observed in soils when the rates of organic matter input to the soil are increased (Stewart et al., 2007; Hassink, 1996). Saturation of recalcitrant C is believed to come from the finite capacity of stabilization mechanisms in soils, such as chemical protection from the decomposition of soil organic matter by clay surfaces (Six et al., 2002). However, the long-term patterns of change in soil C quality and the accumulation pattern of recalcitrant and bioreactive C pools as well as the mechanisms responsible for continuous accumulation or stabilization of soil C reservoirs are poorly known and have not been explicitly integrated into soil biogeochemistry (Luo et al., 2016). Most models of soil C dynamics divide soil organic matter into several conceptual pools and simulate decomposition as a first-order decay process (Luo et al., 2016). As part of this study, we characterized the acid-insoluble and bioreactive soil organic C pools that accumulate following wildfire. The acid-insoluble soil C fraction is assumed to be "recalcitrant" or resistant to biological degradation (Paul et al., 2006; Xu et al., 1997). Hereafter, we define C bioreactivity (C_{BioR}) as the proportion of C mineralized in CO_2 by microbes at constant temperature and constant water content over a long period of time as a relative measure of soil C lability (Laganière et al., 2015; Xu et al., 1997).

Besides its direct role in C cycling, climate has been shown to be an indirect predictor of soil C storage (quantity and accessibility for microbial decomposition) through its effects on geochemistry (Doetterl et al., 2015). In addition, vegetation types determine the quantity, quality and vertical distribution of soil litter inputs, and so lead to differential mechanisms of soil C protection and stabilization (Jobbagy and Jackson, 2000; Laganière et al., 2017), with the moss stratum being a major source of soil C inputs in boreal ecosystems (Preston et al., 2006). Although many of these processes have been investigated separately, we are not aware of any empirical study so far that has quantified all of these processes simultaneously and assessed the relative contribution of climate, time since fire (TSF), vegetation attributes and soil physico-chemistry to soil C_{BioR}.

The objectives of this study are to fill these knowledge gaps by quantifying changes in boreal forest soil C_{BioR} with TSF (from 2 to 314 years), and disentangling the direct and indirect relative contributions of climate, moss dominance, soil particle size distribution and soil chemical properties (pH, exchangeable Mn and Al, and metal oxides) to soil C_{BioR} across the spruce-feather moss bioclimatic domain in eastern North America. Focusing on the complex interplay between climatic and non-climatic factors, and their direct or indirect influence on soil C_{BioR}, we addressed the following questions: i) Does soil C_{BioR} reservoir change with soil organic C accumulation observed with TSF?; and ii) To what extent do direct and indirect relationships among TSF, climate, physico-chemical soil properties and bryophyte dominance influence soil C_{BioR}? We framed our study within the state factor model of ecosystems (Amundson and Jenny, 1997), which emphasizes soil physico-chemical properties understood to be important to the pedogenesis of Podzolic soils (Schaetzl and Anderson, 2005) that occur on the sampled sites. From there, we hypothesized that once site factors such as overstory composition, surficial deposits and soil drainage are accounted for, as they were in the present study: 1) the proportion of soil C_{BioR} increases as forest stands get older, leading to a buildup of soil C_{BioR} under the cold conditions of the boreal forest; 2) alternatively, if the soil C_{BioR} reaches a new equilibrium because of rapid turnover, the proportion of bioreactive C should decline as soil C stocks increase with TSF; and 3) soil C_{BioR} is primarily controlled by TSF and moss dominance in the O layer (FH horizon), and by soil physico-chemistry in the mineral soil.

https://doi.org/10.5194/soil-2019-88
Preprint. Discussion started: 4 December 2019

2 Materials and methods

2.1 Site selection, sampling design and fieldwork

To account for the effects of TSF and climate on soil C pools, we established sample plots across both a chronosequence and a climosequence (Fig. 1; see Andrieux et al. (2018) for a description of the study area). Using numeric forest inventory maps compiled by the Ministère des Forêts, de la Faune et des Parcs du Québec (MFFPQ), we selected stands with as many similaraties as possible in terms of canopy composition (black spruce [*Picea mariana*] stands), surficial deposits (thick till) and mesic drainage conditions. The soils that develop under these conditions typically belong to the Podzolic order (Table 1). Within mesic drainage conditions, soil texture was quite variable (Table 1). These stands were overlaid with fire maps produced by the MFFPQ and other published dendrochronological surveys (Belisle et al., 2011; Bouchard et al., 2008; Cyr et al., 2012; Frégeau et al., 2015; Le Goff et al., 2007; Le Goff et al., 2008; Portier et al., 2016) to establish the chronosequence. We assumed that the black spruce canopy composition did not change significantly with time and that the forest cyclically returned to a black spruce dominance after fire, in so-called recurrent dynamics, as previously described for these forests in a paleological survey (Frégeau et al., 2015). Then, while studying this ecosystem with a single and cyclic successional trajectory and low vegetation diversity, and by carefully selecting stable permanent site conditions, we guarded against pitfall conclusions associated with space–time substitutions when using a chronosequence approach (Walker et al., 2010; Kenkel et al., 1997).

For field inventory and soil sampling, we followed Canada's National Forest Inventory ground plot guidelines (NFI, 2016). Stand biophysical description and soil sampling took place in a single 314 m² circular plot (10 m radius) in each stand. Slope inclination and orientation were recorded from the centre of each plot with a clinometer and a compass, respectively. Every 2 m along two orthogonal transects oriented following the main cardinal directions, and for a total of 20 records per plot, the thickness of the FH horizon was measured on a sample taken with a soil auger, and the dominant moss types (*Sphagnum* spp. or feather mosses) were identified using 400 cm² microplots. After litter and green living mosses were removed, the FH was sampled at the edge of the plot in three 400 cm² microplots that were spaced 15 m from each other, from which we extracted volumetric mineral soil samples (top 15 cm) with a metallic cylinder (ø = 4.7 cm, height = 15 cm). One soil pit was dug at the plot edge and at the same location where we sampled one of the three FH samples, down to the bottom of the podzolic B horizon or to the bedrock when possible, for soil description, and to collect the mineral soil from 15 to 35 cm under the forest floor–mineral soil boundary, as well as in the top 15 cm B horizon with a metallic cylinder (ø = 4.7 cm). The significant stone content at one site prevented us from sampling the mineral soil from 15 to 35 cm, thus, no analyses could be provided for this layer of soil. Samples were kept in the dark and brought to the lab within 15 days for each region. They were kept in the dark at 2°C until processing during the fall.

The fieldwork was conducted in 2015, from 15 June to 8 September. The sampling effort covered 72 sites in black spruce stands where fire had burned 2 to 314 years ago. Climate data were interpolated at the plot level using BioSim v10.3.2 (Régnière et al., 2013) together with 1981–2010 climate normal series (http://climat.meteo.gc.ca/) from surrounding weather stations, and considering local slope attributes measured in the field as correcting factors (Régnière, 1996). Soil characteristics are summarized below (Table 1).

2.2 Laboratory analyses

2.2.1 Soil preparation

First, we prepared a composite of soil materials obtained from every sampled microplot (N = 3), by plot and soil layer (FH or top 15 cm of mineral soil), to create representative samples for each layer in each of the 72 sample plots. FH was sieved through a 6-mm mesh before being oven–dried (60°C), whereas mineral soil samples were dried by air and passed through a 2-mm sieve. Bulk density was determined after weighing the dried samples, assuming there were no coarse fragments in the

https://doi.org/10.5194/soil-2019-88
Preprint. Discussion started: 4 December 2019

FH horizon, and corrected for fragments > 2 mm for the mineral soil. Part of each sample was retained for soil incubation. We used the < 2 mm fraction to determine pH, exchangeable cation and texture (mineral soil only for the latter). Finely ground sub-samples (< 0.5 mm) were used for C concentration, pyrophosphate extractable Fe and Al (B horizon only) and acid hydrolysis analyses.

2.2.2 Soil physico-chemistry

C concentration of each sample was analyzed by dry combustion (Skjemstad and Baldock, 2007) using a Leco TruMac (Leco Corp, St. Joseph, MI, USA). Exchangeable cations were extracted using a Mehlich-3 solution and were analyzed by inductively coupled plasma atomic emission spectroscopy (Ziadi and Sen Tran, 2007), using an Optima 7300 DV (Perkin Elmer Inc., Waltham, MA, USA). Pyrophosphate extractable Fe and Al (i.e., organically complexed metals; Mpy, hereafter defined as metal oxides) were extracted with a 0.1N $Na_4P_2O_7$ solution before analysis with the Optima 7300 DV (Courchesne and Turmel, 2007). FH horizon and mineral soil pH were determined in a soil:water solution by weights of 1:10 and 1:2 (Hendershot and Lalande, 2007), respectively, using a pH meter (Orion 2 Star). Particle size distribution of the mineral soil was assessed using a standard hydrometer method (Kroetsch and Wang, 2007).

2.2.3 Incubation settings

Soil incubation followed the method described in Paré et al. (2011). We prepared a total of 215 microcosms (72 sites x 3 soil layers minus one sample in the 15–35 cm mineral soil). We used 9 g of oven-dried FH and 50 g of air-dried mineral soil. Dried soil was used to ensure that the initial incubation moisture conditions were similar. Soil samples were placed in 100-mL bottom–perforated plastic containers. The containers were previously filled with glass wool (to avoid material losses during moisture adjustments) and pre-washed with HCl (0.1 M) followed by deionized water. The microcosms were saturated with deionized water, drained for 24 hours at 2°C, and weighed to determine their water-holding capacity. Over approximately 50 weeks of experiments, microcosms were placed under constant air temperature (26°C) and humidity (100%) in a growth chamber and, when necessary, deionized water was periodically added to adjust soil moisture to 85% of the water-holding capacity. Except during CO_2 production measurements, each microcosm was stored in a 500-mL Mason jar kept open to maintain aerobic conditions and to prevent CO_2 accumulation to toxic levels. A rubber septum was installed on the metal lid for gas sampling when measuring CO_2 production.

2.2.4 CO_2 production measurements

Carbon dioxide produced by each microcosm was measured periodically (at days 20, 26, 48, 64, 108, 126, 154, 227, 264 and 340 for the FH horizon and at days 8, 14, 21, 29, 36, 43, 51, 57, 72, 79, 86, 101, 113, 140, 203, 238 and 358 for mineral soil layers; Fig. S1), using a LI-6400 portable photosynthesis system (LI-COR®, Lincoln, NE, USA) connected to an N_2 carrier gas (LI-COR® Application Note # 134). The flow rate of the carrier gas was set to 100 $mL.min^{-1}$ using the gas flow meter FMA1812A (Omega Engineering, INC., Norwalk, CO, USA). Initial CO_2 measurements were taken directly after hermetically sealing a jar with a metal lid and final CO_2 measurements were taken after 4 h to 24 h, depending on the soil layer and the progress of the experiment; these measurements were carried out using a 2.5-mL or 10-mL (for FH horizon or mineral soil, respectively) air volume, extracted from the jar headspace with a syringe through the rubber septum. This gas sample was injected through the carrier gas into the LI-6400 infrared analyzer. Carbon dioxide concentration ($\mu mol.mol^{-1}$) was predicted using the linear regression of a sample's measured CO_2 peak against calibration curves obtained from benchmark gas (CO_2 at 800 ppm and 3,000 ppm). The first measurement (initial CO_2 concentration) accounted for the CO_2 concentration of the ambient air when closing the jars. This value was subtracted from the final CO_2 concentration to account solely for the CO_2 produced by the microcosm.

https://doi.org/10.5194/soil-2019-88
Preprint. Discussion started: 4 December 2019

All data were subsequently standardized to a 24-hour period to provide a daily respiration rate and to calculate cumulative C mineralization (Fig. S1) (Paré et al., 2006). In short, we applied the gas law to convert CO_2 concentration (µmol.mol^{-1}) to a C mass basis, using a constant pressure at 101.3 kPa and the specific head space volume of each sample (total volume of the jar minus soil volume and container). Cumulative respiration was calculated according to the following Eq. (1):

$$M_t = M_{t-1} + \frac{(R_t + R_{t-1})}{2} \times (t - t_{-1}), \quad (1)$$

where M_t (mg CO_2-C) is the cumulative mass of C mineralized at time t, R_t (mg CO_2-C.d^{-1}) is the daily respiration rate at time t, and t is the Julian day (d). M_t was divided by the initial C mass (g) of each sample to compute the specific respiration rate (Rs; mg CO_2-C.g$^{-1}C_{org}$). Then, dividing Rs by 10 gave the percentage of initial mass of soil C lost through microbial respiration, or C_{BioR}.

2.2.5 Acid hydrolysis

We used acid hydrolysis as an index of biologically recalcitrant soil C (Xu et al., 1997), which has been proposed as an indicator of a slow-cycling soil C pool (Paul et al., 2006). Hydrolysis was carried out by refluxing 2 g of soil with 50 mL HCl (6M) brought to the boiling point on a hot plate. We used a two-hour reaction time because the majority of soil organic matter is hydrolyzed during the first two hours and longer reaction times do not significantly change C release (Silveira et al., 2008; Xu et al., 1997). Acid-insoluble residues were separated from hydrolysates by filtering the solution on inert paper filters, rinsed three times with 50 mL of deionized water to remove any chlorine residues, oven-dried at 60°C overnight, and weighed before C concentration analysis by dry combustion (see section 2.3.2). Based on the total C concentration of the acid-insoluble residues and mass loss of the samples during the treatments, the hydrolysability (Plante et al., 2006) of a sample was calculated based on the following Eq. (2):

$$C_{AI} = \left(\frac{[C_{AI}] \times M_{AI}}{[C_i] \times M_i}\right) \times 100 \quad (2)$$

where C_{AI} is the percentage of the acid-insoluble C (%), $[C_{AI}]$ and $[C_i]$ are the C concentration of the acid-insoluble residues and of the initial soil (%), and M_{AI} and M_i are the mass of the acid-insoluble residues and of the initial soil sample (g), respectively.

2.3 Ecological *a priori* hypotheses

To address the complex interplay among climatic and non-climatic factors, we first selected the following environmental variables documented in the literature as being important drivers of soil C_{BioR} and pedogenesis of Podzolic soils: climate (temperature and water supply), soil texture, TSF, dominance of the moss functional type, soil pH, and concentration of metal oxides and of exchangeable elements (Mn and Al) (Wiesmeier et al., 2019; Schaetzl and Anderson, 2005). As in other ecosystems (Fierer et al., 2003; Salomé et al., 2010), the boreal forest soil microbial community as well as the chemical and physical environment change with soil depth (Clemmensen et al., 2013; Hynes and Germida, 2013), suggesting different drivers of the decomposition process in FH and mineral soil layers. Hence, for each of the FH and mineral soil layers, we built two separate sets of *a priori* ecological hypotheses expressed as direct acyclic graphs (DAGs) representing different causal relationships among environmental variables and soil C_{BioR} (Fig. 2). Therein, we tested the validity of four competing a priori ecological hypotheses represented by a DAG. This hypothetico-deductive approach, in which each *a priori* hypothesis was supported by ecological knowledge, allows for testing an alternative causal explanation in a falsifiable form as regards the underlying mechanisms of soil C_{BioR} in the two soil layers. For each soil layer, the first hypothesis assumed only direct relationships between environmental variables and soil C_{BioR} (hypotheses FH1 and MIN1 in Fig. 2), such that they mirrored the widespread assumptions used in soil C prediction models based on multiple regression or ANOVA analyses. In addition, framed within Jenny's factor model of soil formation (Jenny, 1994), these baseline hypotheses assumed independence among environmental variables. Alternatively, we formulated *a priori* competing hypotheses in which both direct and indirect effects

https://doi.org/10.5194/soil-2019-88
Preprint. Discussion started: 4 December 2019

among variables and soil C_{BioR} were explicit (hypotheses FH2 and MIN2 in Fig. 2). Justifications for each *a priori* ecological hypothesis are listed below.

2.3.1 Baseline hypothesis for the FH horizon, FH1

This hypothesis assumes that soils that have developed under cooler conditions limiting microbial activity should have a greater C_{BioR} (Laganière et al., 2015) once temperature constraints have been removed. Rainfall under good drainage conditions (such as in this study) should promote greater decomposition rates, and hence lower C_{BioR}. Because wildfire induces polymerization and polycondensation of organic compounds, resulting in residues that are more resistant to biological degradation (Certini, 2005; Gonzalez-Perez et al., 2004; Knicker, 2007), TSF is expected to have a direct and positive effect on C_{BioR} which was anticipated to increase with TSF. Soil pH also had a direct effect on soil bioreactivity because it regulates the microbial community (Fierer and Jackson, 2006) and is a key determinant of the decomposition process (Prescott et al., 2000; Zhang et al., 2008). We expected decreasing C_{BioR} with decreasing pH because acidic soil conditions limit the activity of soil decomposers. Compared to *Sphagnum* spp., feather mosses are more palatable to microbes (Fenton et al., 2010; Lang et al., 2009), so we expected lower C_{BioR} with more Sphagnum. Also, manganese (Mn) availability has been shown to be a good predictor of boreal soil C stocks (Stendahl et al., 2017); hence, Mn being a co-metabolic compound of lignin degradation, we assumed that Mn has a direct positive effect on C_{BioR}.

2.3.2 Alternative hypothesis for the FH horizon, FH2

As in hypothesis FH1, TSF, pH, moss functional type and Mn had direct effects on C bioreactivity. However, this hypothesis differed from FH1 in that TSF and moss dominance also had indirect effects on C_{BioR} through changes in pH conditions. We expected decreasing pH with increasing Sphagnum spp. dominance because some physiological characteristics of these organisms lead to environment acidification (Andrus, 1986). Also, in the short term, fire modifies pH through the liming effect (Gonzalez-Perez et al., 2004; Knicker, 2007). In the long term, soils acidify with TSF as a result of vegetation regrowth, which involves the exchange of protons against cations to maintain the physiological electro-neutrality of the vegetation (Driscoll and Likens, 1982). Contrary to hypothesis FH1, which postulated that climate and soil texture had direct effects on C_{BioR}, hypothesis FH2 assumed that these drivers had only indirect effects on C_{BioR} through their influence on moss dominance.

2.3.3 Baseline hypothesis for the mineral soil, MIN1

This hypothesis assumes that there are only direct effects of environmental variables on C_{BioR} in the mineral soil. Climate and pH directly control the decomposition process. As the binding of organic matter with the mineral phase has been recognized as an important mechanism of C protection against decomposition (Doetterl et al., 2015; Kaiser et al., 2002; Porras et al., 2017), we assumed that there would be direct effects of soil texture and metal oxide contents on C_{BioR}. In the first years following fire, the slow incorporation of charred residues from upper soil layers into the mineral soil could decrease the organic matter quality (Johnson and Curtis, 2001), resulting in a decrease of C_{BioR} with increasing TSF. Mn availability could directly modulate C_{BioR} (see FH1), and exchangeable Al could impede microbial decomposition when in excess (Kunito et al., 2016).

2.3.4 Alternative hypothesis for the mineral soil, MIN2

As an alternative to hypothesis MIN1, this hypothesis assumes that only TSF, pH, metal oxides and Mn/Al have direct effects on C_{BioR}. Additionally, pH is assumed to decrease with TSF because of the imbalance in nutrient uptake caused by aggrading vegetation. Also, exchangeable cations are dependent on pH (Sanborn et al., 2011), and the decrease in pH favours the creation of organometallic complexes impeding microbial decomposition (Buurman and Jongmans, 2005; Porras et al., 2017). Contrary to hypothesis MIN1, which assumed direct effects of climate and soil texture on C_{BioR}, this hypothesis assumes that climate

https://doi.org/10.5194/soil-2019-88
Preprint. Discussion started: 4 December 2019

and soil texture have only indirect effects on C_{BioR}. The indirect effect of climate on C_{BioR} is mediated through its effect on mineral weathering (Doetterl et al., 2015) and the quantity of metal oxides leached from the upper soil layers (Schaetzl and Anderson, 2005). Compared to coarse-textured soils, fine-textured soils have more reactive surface sites that can bind additional Mn and Al ions (Petersen et al., 1996).

2.4 Calculations and data analyses

2.4.1 Index of moss dominance

In order to account for the effects of moss functional traits on C_{BioR} of the FH horizon, we differentiated between *Sphagnum* spp. and feather mosses, since they have different ecophysiological characteristics (Bisbee et al., 2001), e.g., feather mosses decompose faster than Sphagnum spp. (Fenton et al., 2010; Lang et al., 2009). Based on Nalder and Wein (1999), we calculated an index of moss dominance (IMD) using the following Eq. (3):

$$IMD = \frac{O_{sph}}{O_{sph}+O_{pl}+O_{h}+O_{pt}} \quad (3)$$

where *O* is the sum of occurrence of a species in the 20 microplots (see section 2.1), *sph*: *Sphagnum* spp.; *pl*: *Pleurozium schreberi* (Brid.) Mitt.; *h*: *Hylocomium splendens* (Hedw.) Schimp.; *pt*: *Ptilium crista-castrensis* (Hedw.).
Feather mosses dominate the moss stratum when the IMD tends toward 0, whereas *Sphagnum* spp. dominates the moss stratum when the IMD tends toward 1. Some sites (n = 5) that recently had fires did not have any moss species regrowth at the time of the fieldwork. For these sites, we set the IMD to 0.

2.4.2 Soil C quality and bioreactivity

First, we wanted to estimate variation in the size of the soil C pools (bioreactive and recalcitrant) with TSF. For each soil layer (FH, top 15 cm of mineral soil and 15 to 35 cm of mineral soil), we scaled up to plot scale the cumulative proportion of C mineralized at the end of the incubations and the proportion of acid-insoluble C using Eq. (4) and Eq. (5):

$$C_{fast} = C_{BioR} \times D_B \times h \quad (4)$$

$$C_{slow} = C_{AI} \times D_B \times h \quad (5)$$

where C_{fast} and C_{slow} are the bioreactive and recalcitrant soil C pools ($Mg.ha^{-1}$), C_{BioR} is the percentage of initial mass of soil C lost through microbial respiration (%), *DB* is the bulk density ($g.cm^{-3}$), *h* is the soil depth (i.e., mean depth based on 20 measurements per plot for FH; cm) and C_{AI} is the acid-insoluble C fraction (%). Hereafter, the total C stock (C_{tot}), C_{fast} or C_{slow} pool size represents, within each plot, the sum of each C pool across all soil layers.
Secondly, in order to express the qualitative (relative) changes in soil C in relation to environmental variables, we used the proportion of initial mass of soil C lost through microbial respiration as an index of C_{BioR} (see section 2.2.4). In the statistical analyses, we considered the whole mineral soil (in the top 15 cm and in the 15- to 35- cm layer) as a single soil layer by calculating the weighted mean by depth for all mineral soil variables.

2.4.3 Statistical analyses

First, we evaluated post-fire C stock changes in functional reservoirs (bioreactive versus recalcitrant) using the linear regression of C stocks against TSF. Preliminary analyses with generalized additive models and piecewise regressions did not show any significant non-linear or segmented relationships. Secondly, we quantified direct and indirect causal relationships among variables and C_{BioR} using confirmatory path analysis with directional separation tests (Shipley, 2000a), according to the set of alternative *a priori* hypotheses (Fig. 2). Path analysis was used together with Fisher's *C* test (Shipley, 2000b) as a simultaneous test of independence for a model basis set (i.e., all non-adjacent pairs of variables defined as claims of independence). This led us to quantify how our data supported each hypothetical DAG and to identify whether some hypotheses

https://doi.org/10.5194/soil-2019-88
Preprint. Discussion started: 4 December 2019

would be rejected based on a robust statistical test (Shipley, 2009). Fisher's *C* statistic was compared with a χ^2 distribution with 2k degrees of freedom (where k is the number of claims of independence in a model basis set). We rejected a causal model at the significance level $\alpha = 0.05$ when $p < \alpha$. Prior to analyses, we standardized (reduced and centered) all variables to quantify their relative contribution to the variability of soil C_{BioR}.

The fit of each DAG for every soil layer (FH and mineral soil) was compared using a model selection approach together with the second-order Akaike information criterion (AICc) in order to account for small sample sizes (Shipley, 2013). For model selection, we used the relative AICc difference with the "best" model or relative weight (Symonds and Moussalli, 2010). To avoid having latent variables in the models, and because we had no *a priori* knowledge about which specific climate, texture or exchangeable elements should be used for testing the validity of each hypothesis, we used the cross-product of four climatic variables (MAT, GDD5, MAP, WB), three soil texture variables (sand %, silt % and clay %), and two exchangeable elements (Al and Mn, only for mineral soil). Therefore, we tested 12 and 24 model combinations for each hypothesis/DAG involving the FH horizon and the mineral soil, respectively. Given that each soil layer had two alternative causal hypotheses, we then compared 24- and 48-candidate DAG models using a model selection procedure for FH and mineral soil, respectively. Model-averaged estimates were calculated by multiplying each estimate within each model by the corresponding Akaike weight and by summing the resulting values across all models; this allowed all models to influence model-averaged estimates. By doing so, we guarded against making arbitrary decisions about which model should be considered. We used the "ggm" package to compute Fisher's *C* statistic (Marchetti et al., 2015). All calculations and statistics were made using the R software version 3.4.3 (R Core Team, 2017).

3 Results

3.1 Post-fire soil C pool size

Total soil C stock (C_{tot}, i.e., the sum of FH and mineral C stocks in the top 35 cm), the size of the recalcitrant C pool and the size of C_{BioR} pool (C_{slow} and C_{fast}, respectively) all increased linearly with TSF (Fig. 3a). A minimum C_{tot} value of 63 MgC.ha^{-1} was observed for a 100-year-old stand, which is close to the C_{tot} value of 66 MgC.ha^{-1} of the youngest (2-year-old) stand. A maximum C_{tot} value of 305 MgC.ha^{-1} was observed for a 283-year-old stand. On average, C_{slow} size was 6-fold bigger than C_{fast} size (Table 2). C_{fast} values ranged from 5 MgC.ha^{-1} to 25 MgC.ha^{-1} for a 100-year-old stand and for a 91-year-old stand, respectively. C_{slow} values were 29 MgC.ha^{-1} and 175 MgC.ha^{-1} for a 2-year-old stand and for a 91-year-old stand, respectively. Using these simple linear trends, C_{tot} accumulated faster than C_{slow} and C_{fast} ($F_{3,209} = 257.6$, $p < 0.001$; Table 2 and Fig. 3b). Our data indicate that the overall soil C quality did not vary quantitatively with TSF ($R^2 < 0.01$, $p \geq 0.81$ for both C pools; Table 2) because the proportion of C_{slow} and C_{fast} remained constant over the timespan of the fire chronosequence (Fig. 3b).

3.2 FH path analysis and model selection

The causal structure of the baseline hypothesis FH1, which assumes that there are only direct effects of covariates on C_{BioR} in the FH horizon, was rejected for all candidate models (Fisher's *C* statistic > 45, $p < 0.05$; Table 3). Instead, the data better supported the causal structure of alternative hypothesis FH2 for all models (Fisher's *C* statistic < 31, $p > 0.25$; Table 3), which indicates that indirect effects among covariates and C_{BioR} in the FH horizon need to be accounted for in order to properly assess the variation structure in the data. The model selection procedure revealed that the data were best explained by one leading model (hereafter, "best" model; Fisher's *C* statistic = 22.3, $p = 0.67$; Table 3); this model was associated with FH2, with MAP as the climate variable and clay content as the texture variable. The Akaike weight for this model (68%) was about eight times greater than the weight of the second most supported model (8%). The model-averaging procedure revealed that exchangeable Mn and pH of the FH horizon were the two covariates that had the strongest direct and positive effects on C_{BioR} of the FH horizon (both with an averaged path coefficient, pc = 0.34, $p < 0.01$; Fig. 4 and Table S1). TSF was the second most important

https://doi.org/10.5194/soil-2019-88
Preprint. Discussion started: 4 December 2019

relative driver with a significant direct and positive effect on C_{BioR} (pc = 0.24, $p < 0.05$; Fig. 4 and Table S1). Moss dominance had no significant direct effects on C_{BioR} (pc = 0.08, $p > 0.41$; Fig. 4 and Table S1). In addition, both TSF and moss dominance had indirect effects on C_{BioR} through their influences on pH (TSF→pH: pc = -0.32, $p < 0.01$; moss dominance→pH: pc = 0.30, $p < 0.01$; Fig. 4 and Table S1). In addition, the model contained an indirect effect of climate (MAP) on C_{BioR} through its direct and negative effect on moss dominance (pc = -0.25, $p < 0.05$; Fig. 4 and Table S1). We detected no any effect of texture (clay content) of the mineral soil on moss dominance ($-0.01 < pc < 0.05$, $p > 0.43$).

By allowing all of the models (FH1 and FH2) to influence coefficient estimates, the model-averaging procedure indicated that the most important variables exerting a direct control over C_{BioR} of the FH horizon were as follows, by decreasing importance: pH and Mn, TSF, and moss dominance (Table S1). Moreover, we could not detect any direct effect of climatic and texture variables tested in this study on C_{BioR} in the FH horizon.

3.3 Mineral soil path analysis and model selection

The causal structure of the baseline hypothesis MIN1, which assumed that there were only direct effects of covariates on the C_{BioR} of the mineral soil, was rejected (Fisher's *C* statistic > 52, $p < 0.05$; Table 4). Instead, the data best supported the causal structure implied by the alternative hypothesis MIN2 indicating that, similar to the FH horizon, indirect effects among covariates need to be accounted for assessing in order to properly assess variation in the C_{BioR} of the mineral soil. The model selection procedure revealed that the data were best explained by one leading model (hereafter, "best" model; Fisher's *C* statistic = 27.76, p = 0.27; Table 4). This model was associated with MIN2, with WB as the climate variable, clay content as the texture variable, and Al as the exchangeable element variable. The Akaike weight for this model (47%) was about three times greater than for the second most supported model (14%). The model-averaging procedure revealed that exchangeable Al had the strongest direct and negative effect on the C_{BioR} of the mineral soil (pc = -0.32, $p < 0.001$; Fig. 5). Metal oxide content (pc = -0.27, $p < 0.05$) and pH (pc = -0.25, $p < 0.05$) were the second most influential drivers with significant and negative direct effects on the C_{BioR} of the mineral soil. TSF had a small positive direct effect on the C_{BioR} of the mineral soil, but this relationship was not significant (pc = 0.05, $p > 0.36$). In addition, pH induced two indirect effects on the C_{BioR} of the mineral soil, i.e., through its negative and direct effects on Al and Mpy (pH→Al: pc = -0.24, $p < 0.01$; pH→Mpy: pc = -0.34, $p < 0.01$). Clay content had an indirect effect on the C_{BioR} of the mineral soil, through its direct and positive effect on exchangeable Al (pc = 0.17 $p < 0.05$). Also, water balance had a weak indirect effect on the C_{BioR} of the mineral soil through its direct effect on Mpy (pc = 0.11, p = 0.07).

By allowing all the models (MIN1 and MIN2) to influence estimates, the model-averaging procedure indicated that the most important variables tested in this study and exerting a direct control over the C_{BioR} of the mineral soil were as follows, by decreasing importance: exchangeable aluminum, metal oxide contents, pH and TSF (Table S2). Moreover, we failed to detect any direct effect of climate or mineral soil texture on C_{BioR}.

4 Discussion

4.1 Post-fire soil C quality

Most of the studies on post-fire soil C have focused on immediate or short-term responses, and found that fire affects soil C quality by creating profound changes in the structure of soil organic matter compounds through thermal oxidation (Certini, 2005; Gonzalez-Perez et al., 2004). By using a long-term chronosequence of TSF ranging from two to 314 years, our study provides new insights into the understanding of the trajectory of changes in soil C quality following fire, over hundreds of years. Our estimates of the size of fast- and slow-cycling soil C pools and our results indicate that *i)* both pools accumulate with TSF, and *ii)* the proportion of each C pool remains constant with TSF relative to total soil C stock (Fig. 2 and Table 1). These results do not necessarily imply that fire has no effect on soil C functional pools, because our chronosequence has a low

https://doi.org/10.5194/soil-2019-88
Preprint. Discussion started: 4 December 2019

resolution for the first few years following fire, but rather suggest that such changes, if present, are not long-lasting. Our results also highlight that the accumulation process of the bioreactive soil C reservoir does not reach an equilibrium, at least not in the first three centuries following fire. Instead, environmental conditions limiting decomposition, such as cold temperatures under a thickening FH horizon developed with TSF, could have slowed down labile C degradation and allow its accumulation (Kane et al., 2005).

4.2 Control mechanisms of the soil carbon bioreactivity

This study shows that soil C_{BioR} is driven by several climatic and non-climatic variables, some being common both for FH horizon and mineral soil, and others not, suggesting that different mechanisms may be involved in the control of the decomposition process in the FH horizon and in the mineral soil (Shaw et al., 2015;Ziegler et al., 2017).

4.2.1 Soil carbon bioreactivity in the FH horizon

Our results suggested that pH and exchangeable Mn are important drivers of C_{BioR} in the FH horizon. Boreal evergreen coniferous species generate high-lignin litter and forest floor layers (Laganière et al., 2017). This is reflected in the high proportion of acid-insoluble C of FH horizon samples (73 ± 5%, data not shown). Therefore, soil C cycling in boreal forests depends on the capacity of microbes to depolymerize lignin. Microorganisms in the acidic soils of this ecosystem are dominated by fungi that use metalloenzymes–such as Mn peroxidases–to metabolize lignin (Pollegioni et al., 2015), or are white-rot fungi (Basidiomycota) equipped with enzymes that oxidize lignin (Cragg et al., 2015). Soil C stocks in the boreal forest humus layer have been found to be negatively correlated with exchangeable Mn availability (Stendahl et al., 2017). In our study, exchangeable Mn of the FH horizon was positively correlated with C_{BioR}, suggesting that increasing Mn availability stimulates organic matter breakdown and that an Mn bottleneck in soil C cycling may be present (Kranabetter, 2019). We also observed direct and positive causal relationships between pH and C_{BioR} of the FH horizon, indicating that acidic soil conditions limit soil C mineralization (Prescott et al., 2000). Bacterial respiration and microbial community composition were found to be strongly determined by soil pH in the forest soil (Bååth and Anderson, 2003). We found that pH of the FH horizon decreased with TSF. Alongside the direct and positive effect of TSF on C_{BioR} of the FH horizon, our results indicate that dynamic processes constrained by chemical soil properties shifting with stand development after burning (e.g. pH) drive the nature of soil organic matter and potentially the rate of C losses by heterotrophic respiration from boreal forest soils.

Altogether, these results emphasize the need to include both soil chemistry and biological mechanisms into models of soil C cycling to better anticipate the role played by boreal forest in carbon cycle-climate feedbacks. Soil C cycling in mechanistic models of forest C dynamics often assumes that climate drives decay and the transfer rate of and between soil C pools (see Deluca and Boisvenue (2012)). Based on our results, we argue that chemical drivers of soil organic matter decomposition, such as exchangeable Mn concentrations and pH, might be used to modulate soil C dynamics in such models, and we especially advise to accounting for temporal shifts in soil pH occurring with stand development.

We did not detect any direct effect of climate on soil C_{BioR} in the FH horizon. This finding is consistent with the results of unchanged soil C stocks with *in situ* experimental warming worldwide (van Gestel et al., 2018). Furthemore, when synthesizing data of *in situ* experimental warming, Carey et al. (2016) found no changes in the temperature sensitivity of soil respiration at the global biome scale, whereas changes were found to be significant for the boreal biome. The cumulative C mineralization of incubated soils in our study was not modulated by *in situ* temperature, which supports the results of Carey et al. (2016) for their entire dataset, but not for the boreal biome-restricted dataset. However, Carey et al. (2016) did not study soils from the Canadian Boreal Shield.

https://doi.org/10.5194/soil-2019-88
Preprint. Discussion started: 4 December 2019

4.2.2 Soil carbon bioreactivity in the mineral soil

As in the FH layer, our results highlight the role of pH as a regulator of C_{BioR} in the mineral soil. In addition to having a direct effect on C_{BioR}, pH also had two indirect effects. The first indirect effect is through the stimulation of metal oxide production with increasing acidic conditions. We observed that low-pH conditions correlated positively with higher metal oxide contents, which in turn correlated negatively with C_{BioR} in the mineral soil. This result is consistent with previous findings showing the role played by pH in mineral weathering and the preservation of C from decomposition through organo-metal complexation (Andrieux et al., 2018). The second indirect effect of pH on C_{BioR} in the mineral soil is mediated through exchangeable Al only, not through Mn (Table S2). Microbes are vertically stratified within the soil column (Clemmensen et al., 2013; Ekschmitt et al., 2008; Hynes and Germida, 2013), with fungi populating the upper soil layers because of their greater need for metabolic oxygen compared with bacteria, which can more easily dwell in the less-oxygenated deeper soil layers. Our results suggest that, contrary to the FH horizon, oxidative depolymerization of lignin compounds mediated by Mn peroxidases may not be a major process for C cycling in the mineral soil (see above). Instead, the negative effect of pH on exchangeable Al, together with the negative effect of exchangeable Al on C_{BioR} in the mineral soil, indicates that low pH conditions favor a greater exchangeable Al abundance, which in turn impedes organic matter decomposition. These findings are consistent with the observed pH-dependent Al toxicity that slowed microbial catabolic activities in acidic forest soils in Japan (Kunito et al., 2016) and in laboratory experiments (Wood, 1995). Our study goes one step further in that we showing that exchangeable Al content is directly related to soil texture (especially clay content) in these podzolic soils. This supports the hypothesis that exchangeable Al bound to fine mineral particles, such as clay, might act as a source of stored Al that can be mobilized and complexed with C to impede decomposition.

Contrary to the FH horizon, we found that TSF was only weakly correlated to mineral soil C_{BioR} and pH, and these relationships were not significant. We also found that the indirect effect of climate (correlation between water balance and metal oxides) on C_{BioR} was marginal. These results indicate that effects of TSF (direct and indirect) and water availability (indirect) on C_{BioR} are restricted to surface organic horizons. Our results support the idea that properties of the organic layer are more likely to be affected by fire because they are directly exposed to surface heating (De Bano, 1990), and that the thick humus layer of boreal forest soils (Table 1) protects deeper soil layers from shifts in environmental conditions. The fact that black spruce roots mostly develop in the top soil (Yuan and Chen, 2010) could explain why we did not observe shifts in pH of the mineral soil with TSF.

5 Conclusion

Theoretically, soil carbon dynamics can be predicted through a knowledge of soil carbon pool sizes, changes in inputs, and sensitivity to environmental factors (Luo et al., 2016). Understanding the bioreactivity of the large boreal forest soils C reservoir is key to predicting future global C cycle in the face of global warming. Some factors may act as C stabilization agents of soil C (i.e., metal oxides binding organic matter), while others may contribute to accelerating or slowing down the rate of soil organic matter biological processing (i.e., exchangeable Mn as a co-metabolic compound of lignin degradation; when in excess, toxicity of exchangeable Al for microbes; soil acidity regulating the microbial activity), and finally, others are related to the quality of organic matter inputs to the soil (i.e., type of moss flora; low-quality organic materials left after fire) or simply to the time require by the system to adjust and reach steady-state (i.e., causal relationships between time since fire and pH, or pH and metal oxides). Our "best" models showed that the climatic conditions experienced *in situ*, expressed here as temperature and water availability, had no direct effect on *in vitro* soil C_{BioR}. Moreover, the indirect effects of climate on soil C_{BioR} are limited to water supply factors, not to temperature. "Best" models also reveal direct and indirect effects on C_{BioR} of both site properties and factors that evolve with TSF. Understanding and predicting changes in soil chemistry is therefore a key challenge that remains to be addressed in future works in order to improve our understanding of soil C balance with global change. Our results are in agreement with Davidson and Janssens (2006) and Davidson (2015), suggesting that improvements

https://doi.org/10.5194/soil-2019-88
Preprint. Discussion started: 4 December 2019

to ESMs may arise from integrating the long-term effects of climate on soil properties with the environmental constraints on microbiological degradation of soil organic matter.

The results of this study identified new pathways for the control mechanisms of soil C_{BioR} that could help to predict the response of boreal forest soils to global change. While earth system models (ESMs) commonly focus on a temperature dependence of soil C decomposition (Bradford et al., 2016), our study showed, in agreement with Rasmussen et al. (2018), that key soil properties, because of their relationship to soil C bioreactivity, could improve ESMs for modeling soil C dynamics in relation to climate change. In particular, our study shows that predictive models need to include the direct effects of soil chemistry and the indirect effects of climate and soil texture on soil C_{BioR}. Moreover, while some factors (metal oxides, TSF) were found to affect both soil C_{BioR} (this study) and soil C stocks (Andrieux et al., 2018), at the same time, other factors did not have such effects (types of mosses, pH). For example, moss dominance had a direct effect on C stock (Andrieux et al., 2018), but not on C_{BioR} (this study) in the FH horizon.

The path analyses and model selection procedure used in our study have made it possible to distinguish direct from indirect effects of ecological drivers on soil C dynamics. We found that the local climate shaped soil C_{BioR} indirectly through effects on moss dominance and on metal oxides, and that of the four climatic variables examined, only the variables related to water supply–and not temperature–significantly but indirectly affected soil C_{BioR}. This suggests that the forecasted increase of 11% precipitation by the end of this century in eastern North America (IPCC, 2013) would indirectly modulate soil C stocks (Andrieux et al., 2018) and soil C_{BioR} (this study), together with the indirect effects of climate on the mechanisms of soil C stock and bioreactivity. How the boreal ecosystem C balance will evolve in the context of global change might be assessed through further research focusing on the changes in soil physico-chemical reactions pertaining to the mechanisms of soil organic matter decomposition and stabilization (Thornley and Canell, 2001).

Data availability

All data presented in this paper can be accessed online free of charge on Canada's Open Government website (https://open.canada.ca, DOI to be determined).

Author contribution

BA, DP, YB and PG participated in writing the funding application and in designing the study. BA and PG did the fieldwork. BA and DP contributed to the lab work. BA and JB analyzed the data. BA prepared the manuscript with contributions from all co-authors.

Competing of interest

The authors declare that they have no conflict of interest.

Acknowledgements

This project was funded by Mitacs Acceleration grants IT05018 (FR11062 to FR11067). We would like to thank Catherine Bruyère, Cécile Remy, Arnaud Guillemard and Eric Beaulieu for field assistance. We are grateful to Danielle Charron and Pierre Clouâtre for helping with field logistics. We warmly thank Véronique Poirier, Jean Noël and Emeline Chaste for help with geomatics work, and Serge Rousseau for laboratory analyses as well as Cindy Shaw for insightful comments. We declare that we have no conflicts of interest.

https://doi.org/10.5194/soil-2019-88
Preprint. Discussion started: 4 December 2019

References

Amundson, R., and Jenny, H.: On a state factor model of ecosystems, BioScience, 47, 536-543, 10.2307/1313122, 1997.

Andrieux, B., Beguin, J., Bergeron, Y., Grondin, P., and Paré, D.: Drivers of post-fire organic carbon accumulation in the boreal forest, Global Change Biology, 10.1111/gcb.14365, 2018.

Andrus, R. E.: Some aspects of Sphagnum ecology, Canadian Journal of Botany, 64, 416-426, 10.1139/b86-057, 1986.

Bååth, E., and Anderson, T. H.: Comparison of soil fungal/bacterial ratios in a pH gradient using physiological and PLFA-based techniques, Soil Biology and Biochemistry, 35, 955-963, 10.1016/s0038-0717(03)00154-8, 2003.

Belisle, A. C., Gauthier, S., Cyr, D., Bergeron, Y., and Morin, H.: Fire regime and old-growth boreal forests in central Quebec, Canada: An ecosystem management perspective, Silva Fenn, 45, 889-908, 2011.

Bisbee, K., Gower, S., Norman, J., and Nordheim, E.: Environmental controls on ground cover species composition and productivity in a boreal black spruce forest, Oecologia, 129, 261-270, 10.1007/s004420100719, 2001.

Bond-Lamberty, B., Peckham, S. D., Ahl, D. E., and Gower, S. T.: Fire as the dominant driver of central Canadian boreal forest carbon balance, Nature, 450, 89-92, 10.1038/nature06272, 2007.

Bouchard, M., Pothier, D., and Gauthier, S.: Fire return intervals and tree species succession in the North Shore region of eastern Quebec, Canadian Journal of Forest Research, 38, 1621-1633, 10.1139/x07-201, 2008.

Bradford, M. A., Wieder, W. R., Bonan, G. B., Fierer, N., Raymond, P. A., and Crowther, T. W.: Managing uncertainty in soil carbon feedbacks to climate change, Nature Climate Change, 6, 751-758, 10.1038/nclimate3071, 2016.

Buurman, P., and Jongmans, A. G.: Podzolisation and soil organic matter dynamics, Geoderma, 125, 71-83, 10.1016/j.geoderma.2004.07.006, 2005.

Carey, J. C., Tang, J., Templer, P. H., Kroeger, K. D., Crowther, T. W., Burton, A. J., Dukes, J. S., Emmett, B., Frey, S. D., Heskel, M. A., Jiang, L., Machmuller, M. B., Mohan, J., Panetta, A. M., Reich, P. B., Reinsch, S., Wang, X., Allison, S. D., Bamminger, C., Bridgham, S., Collins, S. L., de Dato, G., Eddy, W. C., Enquist, B. J., Estiarte, M., Harte, J., Henderson, A., Johnson, B. R., Larsen, K. S., Luo, Y., Marhan, S., Melillo, J. M., Penuelas, J., Pfeifer-Meister, L., Poll, C., Rastetter, E., Reinmann, A. B., Reynolds, L. L., Schmidt, I. K., Shaver, G. R., Strong, A. L., Suseela, V., and Tietema, A.: Temperature response of soil respiration largely unaltered with experimental warming, Proceedings of the National Academy of Sciences of the United States of America, 113, 13797-13802, 10.1073/pnas.1605365113, 2016.

Certini, G.: Effects of fire on properties of forest soils: a review, Oecologia, 143, 1-10, 10.1007/s00442-004-1788-8, 2005.

Chaste, E., Girardin, M. P., Kaplan, J. O., Portier, J., Bergeron, Y., and Hély, C.: The pyrogeography of eastern boreal Canada from 1901 to 2012 simulated with the LPJ-LMfire model, Biogeosciences, 15, 1273-1292, 10.5194/bg-15-1273-2018, 2018.

Clemmensen, K. E., Bahr, A., Ovaskainen, O., Dahlberg, A., Ekblad, A., Wallander, H., Stenlid, J., Finlay, R. D., Wardle, D. A., and Lindahl, B. D.: Roots and associated fungi drive long-term carbon sequestration in boreal forest, Science, 339, 1615-1618, 10.1126/science.1231923, 2013.

Cotrufo, M. F., Wallenstein, M. D., Boot, C. M., Denef, K., and Paul, E.: The Microbial Efficiency-Matrix Stabilization (MEMS) framework integrates plant litter decomposition with soil organic matter stabilization: do labile plant inputs form stable soil organic matter?, Global change biology, 19, 988-995, 10.1111/gcb.12113, 2013.

Courchesne, F., and Turmel, M.-C.: Extractable Al, Fe, Mn, and Si, in: Soil Sampling and Methods of Analysis, Second Edition, edited by: Carter M. R., and Gregorich, E. G., CRC Press, Boca Raton, FL, 2007.

Cragg, S. M., Beckham, G. T., Bruce, N. C., Bugg, T. D., Distel, D. L., Dupree, P., Etxabe, A. G., Goodell, B. S., Jellison, J., McGeehan, J. E., McQueen-Mason, S. J., Schnorr, K., Walton, P. H., Watts, J. E., and Zimmer, M.: Lignocellulose degradation mechanisms across the Tree of Life, Current opinion in chemical biology, 29, 108-119, 10.1016/j.cbpa.2015.10.018, 2015.

Craine, J. M., Fierer, N., and McLauchlan, K. K.: Widespread coupling between the rate and temperature sensitivity of organic matter decay, Nature Geoscience, 3, 854-857, 10.1038/ngeo1009, 2010.

Cyr, D., Gauthier, S., and Bergeron, Y.: The influence of landscape-level heterogeneity in fire frequency on canopy composition in the boreal forest of eastern Canada, J Veg Sci, 23, 140-150, DOI 10.1111/j.1654-1103.2011.01338.x, 2012.

https://doi.org/10.5194/soil-2019-88
Preprint. Discussion started: 4 December 2019

Davidson, E. A., and Janssens, I. A.: Temperature sensitivity of soil carbon decomposition and feedbacks to climate change, Nature, 440, 165-173, 10.1038/nature04514, 2006.
Davidson, E. A.: Soil carbon in a beer can, Nature Geoscience, 8, 748-749, 10.1038/ngeo2522, 2015.
De Bano, L. F.: The effect of fire on soil properties, Management and Productivity of Western-Montane Forest Soils, Boise, 1990.
Deluca, T. H., and Boisvenue, C.: Boreal forest soil carbon: distribution, function and modelling, Forestry, 85, 161-184, 10.1093/forestry/cps003, 2012.
Doetterl, S., Stevens, A., Six, J., Merckx, R., Van Oost, K., Casanova Pinto, M., Casanova-Katny, A., Muñoz, C., Boudin, M., Zagal Venegas, E., and Boeckx, P.: Soil carbon storage controlled by interactions between geochemistry and climate, Nature Geoscience, 8, 780-783, 10.1038/ngeo2516, 2015.
Driscoll, C. T., and Likens, G. E.: Hydrogen ion budget of an aggrading forested ecosystem, Tellus, 34, 283-292, 10.1111/j.2153-3490.1982.tb01817.x, 1982.
Ekschmitt, K., Kandeler, E., Poll, C., Brune, A., Buscot, F., Friedrich, M., Gleixner, G., Hartmann, A., Kästner, M., Marhan, S., Miltner, A., Scheu, S., and Wolters, V.: Soil-carbon preservation through habitat constraints and biological limitations on decomposer activity, Journal of Plant Nutrition and Soil Science, 171, 27-35, 10.1002/jpln.200700051, 2008.
Fenton, N. J., Bergeron, Y., and Paré, D.: Decomposition rates of bryophytes in managed boreal forests: influence of bryophyte species and forest harvesting, Plant and Soil, 336, 499-508, 10.1007/s11104-010-0506-z, 2010.
Fierer, N., Allen, A. S., Schimel, J. P., and Holden, P. A.: Controls on microbial CO_2 production: a comparison of surface and subsurface soil horizons, Global Change Biology, 9, 1322-1332, 10.1046/j.1365-2486.2003.00663.x, 2003.
Fierer, N., Craine, J. M., McLauchlan, K., and Schimel, J. P.: Litter Quality and the Temperature Sensitivity of Decomposition, Ecology, 86, 320-326, 10.1890/04-1254, 2005.
Fierer, N., and Jackson, R. B.: The diversity and biogeography of soil bacterial communities, Proceedings of the National Academy of Sciences of the United States of America, 103, 626-631, 10.1073/pnas.0507535103, 2006.
Frégeau, M., Payette, S., and Grondin, P.: Fire history of the central boreal forest in eastern North America reveals stability since the mid-Holocene, The Holocene, 25, 1912-1922, 10.1177/0959683615591361, 2015.
Gonzalez-Perez, J. A., Gonzalez-Vila, F. J., Almendros, G., and Knicker, H.: The effect of fire on soil organic matter--a review, Environment international, 30, 855-870, 10.1016/j.envint.2004.02.003, 2004.
Hassink, J.: Preservation of Plant Residues in Soils Differing in Unsaturated Protective Capacity, Soil Science Society of America Journal, 60, 10.2136/sssaj1996.03615995006000020021x, 1996.
Hendershot, W. H., and Lalande, H.: Soil Reaction and Exchangeable Acidity, in: Soil Sampling and Methods of Analysis, Second Edition, edited by: Carter M. R., and Gregorich, E. G., CRC Press, Boca Raton, FL, 2007.
Hynes, H. M., and Germida, J. J.: Impact of clear cutting on soil microbial communities and bioavailable nutrients in the LFH and Ae horizons of Boreal Plain forest soils, Forest Ecology and Management, 306, 88-95, 10.1016/j.foreco.2013.06.006, 2013.
IPCC: Climate change 2013: the physical science basis. Contribution of Working Group I to the Fifth Assessment Report of the Intergovernmental Panel on Climate Change, Cambridge University Press, Cambridge, UK and New York, NY, 1535 pp., 2013.
IUSS Working Group WRB: World reference base for soil resources 2014, update 2015. International soil classification system for naming soils and creating legends for soil maps., World Soil Resources Reports, FAO, Rome, 2015.
Jenny, H.: Factors of soil formation: a system of quantitative pedology, Dover Publications Inc., New York, NY, 1994.
Jobbagy, E. G., and Jackson, R. B.: The vertical distribution of soil organic carbon and its relation to climate and vegetation, Ecological Applications, 10, 423-436, 10.2307/2641104, 2000.
Johnson, D. W., and Curtis, P. S.: Effects of forest management on soil C and N storage: meta analysis, Forest Ecology and Management, 140, 227-238, 10.1016/S0378-1127(00)00282-6, 2001.
Kaiser, K., Eusterhues, K., Rumpel, C., Guggenberger, G., and Kögel-Knabner, I.: Stabilization of organic matter by soil minerals — investigations of density and particle-size fractions from two acid forest soils, Journal of Plant Nutrition and Soil Science, 165, 451, 10.1002/1522-2624(200208)165:4<451::aid-jpln451>3.0.co;2-b, 2002.
Kane, E. S., Valentine, D. W., Schuur, E. A., and Dutta, K.: Soil carbon stabilization along climate and stand productivity gradients in black spruce forests of interior Alaska, Canadian Journal of Forest Research, 35, 2118-2129, 10.1139/x05-093, 2005.

Kenkel, N. C., Walker, D. J., Watson, P. R., Caners, R. T., and Lastra, R. A.: Vegetation dynamics in boreal forest ecosystems, Coenoses, 12, 97-108, 1997.
Knicker, H.: How does fire affect the nature and stability of soil organic nitrogen and carbon? A review, Biogeochemistry, 85, 91-118, 10.1007/s10533-007-9104-4, 2007.
Kranabetter, J. M.: Increasing soil carbon content with declining soil manganese in temperate rainforests: is there a link to fungal Mn?, Soil Biology and Biochemistry, 128, 179-181, 10.1016/j.soilbio.2018.11.001, 2019.
Kroetsch, D., and Wang, C.: Particle Size Distribution, in: Soil Sampling and Methods of Analysis, Second Edition, edited by: Carter M. R., and Gregorich, E. G., CRC Press, Boca Raton, FL, 2007.
Kunito, T., Isomura, I., Sumi, H., Park, H.-D., Toda, H., Otsuka, S., Nagaoka, K., Saeki, K., and Senoo, K.: Aluminum and acidity suppress microbial activity and biomass in acidic forest soils, Soil Biology and Biochemistry, 97, 23-30, 10.1016/j.soilbio.2016.02.019, 2016.
Kurz, W. A., Shaw, C. H., Boisvenue, C., Stinson, G., Metsaranta, J., Leckie, D., Dyk, A., Smyth, C., and Neilson, E. T.: Carbon in Canada's boreal forest — A synthesis, Environmental Reviews, 21, 260-292, 10.1139/er-2013-0041, 2013.
Laganière, J., Podrebarac, F., Billings, S. A., Edwards, K. A., and Ziegler, S. E.: A warmer climate reduces the bioreactivity of isolated boreal forest soil horizons without increasing the temperature sensitivity of respiratory CO2 loss, Soil Biology and Biochemistry, 84, 177-188, 10.1016/j.soilbio.2015.02.025, 2015.
Laganière, J., Boča, A., Van Miegroet, H., and Paré, D.: A tree species effect on soil that is consistent across the species' range: The case of aspen and soil carbon in North America, Forests, 8, 113, 10.3390/f8040113, 2017.
Lang, S. I., Cornelissen, J. H. C., Klahn, T., van Logtestijn, R. S. P., Broekman, R., Schweikert, W., and Aerts, R.: An experimental comparison of chemical traits and litter decomposition rates in a diverse range of subarctic bryophyte, lichen and vascular plant species, Journal of Ecology, 97, 886-900, 10.1111/j.1365-2745.2009.01538.x, 2009.
Le Goff, H., Flannigan, M. D., Bergeron, Y., and Girardin, M. P.: Historical fire regime shifts related to climate teleconnections in the Waswanipi area, central Quebec, Canada, International Journal of Wildland Fire, 16, 607-618, 10.1071/Wf06151, 2007.
Le Goff, H., Girardin, M. P., Flannigan, M., and Bergeron, Y.: Dendroclimatic inference of wildfire activity in Quebec over the 20th century and implication for natural disturbance-based forest management at the northern limit of the commercial forest, International Journal of Wildland Fire, 17, 348-362, 2008.
Luo, Y., Ahlström, A., Allison, S. D., Batjes, N. H., Brovkin, V., Carvalhais, N., Chappell, A., Ciais, P., Davidson, E. A., Finzi, A., Georgiou, K., Guenet, B., Hararuk, O., Harden, J. W., He, Y., Hopkins, F., Jiang, L., Koven, C., Jackson, R. B., Jones, C. D., Lara, M. J., Liang, J., McGuire, A. D., Parton, W., Peng, C., Randerson, J. T., Salazar, A., Sierra, C. A., Smith, M. J., Tian, H., Todd-Brown, K. E. O., Torn, M., van Groenigen, K. J., Wang, Y. P., West, T. O., Wei, Y., Wieder, W. R., Xia, J., Xu, X., Xu, X., and Zhou, T.: Toward more realistic projections of soil carbon dynamics by Earth system models, Global Biogeochemical Cycles, 30, 40-56, 10.1002/2015gb005239, 2016.
Nalder, I. A., and Wein, R. W.: Long-term forest floor carbon dynamics after fire in upland boreal forests of western Canada, Global Biogeochemical Cycles, 13, 951-968, 10.1029/1999gb900056, 1999.
Canada's national forest inventory: nfi.nfis.org, 2016.
Paré, D., Boutin, R., Larocque, G. R., and Raulier, F.: Effect of temperature on soil organic matter decomposition in three forest biomes of eastern Canada, Canadian Journal of Soil Science, 86, 247-256, 10.4141/s05-084, 2006.
Paré, D., Banville, J. L., Garneau, M., and Bergeron, Y.: Soil Carbon Stocks and Soil Carbon Quality in the Upland Portion of a Boreal Landscape, James Bay, Quebec, Ecosystems, 14, 533-546, 10.1007/s10021-011-9429-7, 2011.
Paul, E. A., Morris, S. J., Conant, R. T., and Plante, A. F.: Does the Acid Hydrolysis–Incubation Method Measure Meaningful Soil Organic Carbon Pools?, Soil Science Society of America Journal, 70, 1023, 10.2136/sssaj2005.0103, 2006.
Petersen, L. W., Moldrup, P., Jacobsen, O. H., and Rolston, D. E.: Relations between Specific Surface Area and Soil Physical and Chemical Properties, Soil Science, 161, 9-21, 10.1097/00010694-199601000-00003, 1996.
Plante, A. F., Conant, R. T., Paul, E. A., Paustian, K., and Six, J.: Acid hydrolysis of easily dispersed and microaggregate-derived silt- and clay-sized fractions to isolate resistant soil organic matter, European Journal of Soil Science, 57, 456-467, 10.1111/j.1365-2389.2006.00792.x, 2006.
Pollegioni, L., Tonin, F., and Rosini, E.: Lignin-degrading enzymes, The FEBS journal, 282, 1190-1213, 10.1111/febs.13224, 2015.

https://doi.org/10.5194/soil-2019-88
Preprint. Discussion started: 4 December 2019

Porras, R. C., Hicks Pries, C. E., McFarlane, K. J., Hanson, P. J., and Torn, M. S.: Association with pedogenic iron and aluminum: effects on soil organic carbon storage and stability in four temperate forest soils, Biogeochemistry, 133, 333-345, 10.1007/s10533-017-0337-6, 2017.

Portier, J., Gauthier, S., Leduc, A., Arseneault, D., and Bergeron, Y.: Fire regime along latitudinal gradients of continuous to discontinuous coniferous boreal forests in eastern Canada, Forests, 7, 211, 10.3390/f7100211, 2016.

Prescott, C. E., Maynard, D. G., and Laiho, R.: Humus in northern forests: friend or foe?, Forest Ecology and Management, 133, 23-36, 10.1016/s0378-1127(99)00295-9, 2000.

Preston, C. M., Bhatti, J. S., Flanagan, L. B., and Norris, C.: Stocks, chemistry, and sensitivity to climate change of dead organic matter along the Canadian boreal forest transect case study, Climatic Change, 74, 223-251, 10.1007/s10584-006-0466-8, 2006.

Rasmussen, C., Heckman, K., Wieder, W. R., Keiluweit, M., Lawrence, C. R., Berhe, A. A., Blankinship, J. C., Crow, S. E., Druhan, J. L., Hicks Pries, C. E., Marin-Spiotta, E., Plante, A. F., Schädel, C., Schimel, J. P., Sierra, C. A., Thompson, A., and Wagai, R.: Beyond clay: towards an improved set of variables for predicting soil organic matter content, Biogeochemistry, 137, 297-306, 10.1007/s10533-018-0424-3, 2018.

Régnière, J.: Generalized Approach to Landscape-Wide Seasonal Forecasting with Temperature-Driven Simulation Models, Environmental Entomology, 25, 869-881, 10.1093/ee/25.5.869, 1996.

Régnière, J., Saint-Amant, R., and Béchard, A.: *BioSIM 10 user's manual*, Natural Resources Canada, Québec, QC, 2013.

Salomé, C., Nunan, N., Pouteau, V., Lerch, T. Z., and Chenu, C.: Carbon dynamics in topsoil and in subsoil may be controlled by different regulatory mechanisms, Global Change Biology, 16, 416-426, 10.1111/j.1365-2486.2009.01884.x, 2010.

Sanborn, P., Lamontagne, L., and Hendershot, W.: Podzolic soils of Canada: Genesis, distribution, and classification, Canadian Journal of Soil Science, 91, 843-880, 10.4141/Cjss10024, 2011.

Schaetzl, R., and Anderson, S.: Soils: genesis and geomorphology 2ed., Cambridge University Press, New York, 817 pp., 2005.

Scharlemann, J. P. W., Tanner, E. V. J., Hiederer, R., and Kapos, V.: Global soil carbon: understanding and managing the largest terrestrial carbon pool, Carbon Management, 5, 81-91, 10.4155/cmt.13.77, 2014.

Schmidt, M. W., Torn, M. S., Abiven, S., Dittmar, T., Guggenberger, G., Janssens, I. A., Kleber, M., Kogel-Knabner, I., Lehmann, J., Manning, D. A., Nannipieri, P., Rasse, D. P., Weiner, S., and Trumbore, S. E.: Persistence of soil organic matter as an ecosystem property, Nature, 478, 49-56, 10.1038/nature10386, 2011.

Shaw, C. H., Hilger, A. B., Metsaranta, J., Kurz, W. A., Russo, G., Eichel, F., Stinson, G., Smyth, C., and Filiatrault, M.: Evaluation of simulated estimates of forest ecosystem carbon stocks using ground plot data from Canada's National Forest Inventory, Ecological Modelling, 272, 323-347, 10.1016/j.ecolmodel.2013.10.005, 2014.

Shaw, C. H., Bona, K. A., Kurz, W. A., and Fyles, J. W.: The importance of tree species and soil taxonomy to modeling forest soil carbon stocks in Canada, Geoderma Regional, 4, 114-125, 10.1016/j.geodrs.2015.01.001, 2015.

Shipley, B.: Cause and correlation in biology: a user's guide to path analysis, structural equations and causal inference, Cambridge University Press, Cambridge, UK, 2000a.

Shipley, B.: A new inferential test for path models based on directed acyclic graphs, Structural Equation Modeling, 7, 206-218, 10.1207/s15328007sem0702_4, 2000b.

Shipley, B.: Confirmatory path analysis in a generalized multilevel context, Ecology, 90, 363-368, 10.1890/08-1034.1, 2009.

Shipley, B.: The AIC model selection method applied to path analytic models compared using a d-separation test, Ecology, 94, 560-564, 10.1890/12-0976.1, 2013.

Silveira, M. L., Comerford, N. B., Reddy, K. R., Cooper, W. T., and El-Rifai, H.: Characterization of soil organic carbon pools by acid hydrolysis, Geoderma, 144, 405-414, 10.1016/j.geoderma.2008.01.002, 2008.

Six, J., Conant, R. T., Paul, E. A., and Paustian, K.: Stabilization mechanisms of soil organic matter: Implications for C-saturation of soils, Plant and Soil, 241, 155-176, 10.1023/a:1016125726789, 2002.

Skjemstad, J. O., and Baldock, J. A.: Total and Organic Carbon, in: Soil Sampling and Methods of Analysis, Second Edition, edited by: Carter M. R., and Gregorich, E. G., CRC Press, Boca Raton, FL, 2007.

Stendahl, J., Berg, B., and Lindahl, B. D.: Manganese availability is negatively associated with carbon storage in northern coniferous forest humus layers, Scientific reports, 7, 15487, 10.1038/s41598-017-15801-y, 2017.

Stewart, C. E., Paustian, K., Conant, R. T., Plante, A. F., and Six, J.: Soil carbon saturation: concept, evidence and evaluation, Biogeochemistry, 86, 19-31, 10.1007/s10533-007-9140-0, 2007.

https://doi.org/10.5194/soil-2019-88
Preprint. Discussion started: 4 December 2019

Symonds, M. R. E., and Moussalli, A.: A brief guide to model selection, multimodel inference and model averaging in behavioural ecology using Akaike's information criterion, Behavioral Ecology and Sociobiology, 65, 13-21, 10.1007/s00265-010-1037-6, 2010.
Thornley, J. H. M., and Canell, M. G. R.: Soil carbon storage response to temperature: an hypothseis, Annals of Botany, 87, 591-598, 10.1006/anbo.2001.1372, 2001.
van Gestel, N., Shi, Z., van Groenigen, K. J., Osenberg, C. W., Andresen, L. C., Dukes, J. S., Hovenden, M. J., Luo, Y., Michelsen, A., Pendall, E., Reich, P. B., Schuur, E. A. G., and Hungate, B. A.: Predicting soil carbon loss with warming, Nature, 554, E4-E5, 10.1038/nature25745, 2018.
Walker, L. R., Wardle, D. A., Bardgett, R. D., and Clarkson, B. D.: The use of chronosequences in studies of ecological succession and soil development, Journal of Ecology, 98, 725-736, 10.1111/j.1365-2745.2010.01664.x, 2010.
Wiesmeier, M., Urbanski, L., Hobley, E., Lang, B., von Lützow, M., Marin-Spiotta, E., van Wesemael, B., Rabot, E., Ließ, M., Garcia-Franco, N., Wollschläger, U., Vogel, H.-J., and Kögel-Knabner, I.: Soil organic carbon storage as a key function of soils - A review of drivers and indicators at various scales, Geoderma, 333, 149-162, 10.1016/j.geoderma.2018.07.026, 2019.
Wood, M.: A mechanism of aluminium toxicity to soil bacteria and possible ecological implications, Plant and Soil, 171, 63-69, 10.1007/bf00009566, 1995.
Xu, J. M., Cheng, H. H., Koskinen, W. C., and Molina, J. A. E.: Characterization of potentially bioreactive soil organic carbon and nitrogen by acid hydrolysis, Nutrient Cycling in Agroecosystems, 49, 267-271, 10.1023/a:1009763023828, 1997.
Yuan, Z. Y., and Chen, H. Y. H.: Fine Root Biomass, Production, Turnover Rates, and Nutrient Contents in Boreal Forest Ecosystems in Relation to Species, Climate, Fertility, and Stand Age: Literature Review and Meta-Analyses, Critical Reviews in Plant Sciences, 29, 204-221, 10.1080/07352689.2010.483579, 2010.
Zhang, D., Hui, D., Luo, Y., and Zhou, G.: Rates of litter decomposition in terrestrial ecosystems: global patterns and controlling factors, Journal of Plant Ecology, 1, 85-93, 10.1093/jpe/rtn002, 2008.
Ziadi, N., and Sen Tran, T.: Mehlich 3-Extractable Elements, in: Soil Sampling and Methods of Analysis, Second Edition, edited by: Carter M. R., and Gregorich, E. G., CRC Press, Boca Raton, FL, 2007.
Ziegler, S. E., Benner, R., Billings, S. A., Edwards, K. A., Philben, M., Zhu, X., and Laganière, J.: Climate warming can accelerate carbon fluxes without changing soil carbon stocks, Frontiers in Earth Science, 5, 10.3389/feart.2017.00002, 2017.

https://doi.org/10.5194/soil-2019-88
Preprint. Discussion started: 4 December 2019

Table 1: General characteristics of the sampling sites.

Variable		Minimum	Maximum	Mean (± sd)
Mean annual temperature (°C)		-2.8	0.7	-0.5 (± 0.8)
Growing degree-day above 5°C (°C)		838	1,290	1,110 (± 110)
Mean annual precipitation (mm)		861	1,027	934 (± 52)
Water balance (mm)		493	660	558 (± 46)
FH depth (cm)		9.8	49.3	22.6 (± 8.4)
Soil thickness (cm)		10	103	39 (± 15)
pH	FH horizon (O layer)	3.3	4.2	3.7 (± 0.2)
	Mineral soil (top 15 cm)	4.2	5.6	4.7 (± 0.2)
	Mineral soil (from 15 to 35 cm)	4.5	5.9	5.2 (± 0.3)
Bulk density	FH horizon	0.05	0.15	0.08 (± 0.02)
	Mineral soil (top 15 cm)	0.73	1.6	1.06 (± 0.18)
	Mineral soil (from 15 to 35 cm)	0.59	1.45	1.02 (± 0.21)
Particle size (%)	Sand	26	92	70 (± 11)
	Silt	5	63	24 (± 10)
	Clay	2	22	6 (± 3)
Soil group[a]			Podzol	

[a]According to IUSS Working Group WRB (2015).

Table 2: Post-fire soil C pool size and accumulation rates.

		Mean (± sd)	Equation	R^2	p-value
C_{tot}	$MgC.ha^{-1}$	150.80 (± 49.91)	120.32 + 0.280*TSF[a]	0.20	**< 0.001**
C_{slow}	$MgC.ha^{-1}$	69.01 (± 25.79)	56.16 + 0.118*TSF	0.14	**0.002**
	% of C_{tot}	46.40 (± 9.35)	46.74 - 0.003*TSF	< 0.01	0.808
C_{fast}	$MgC.ha^{-1}$	11.47 (± 3.59)	9.25 + 0.020*TSF	0.21	**< 0.001**
	% of C_{tot}	7.85 (± 1.67)	7.87 – 0.0002*TSF	<0.01	0.935

[a]TSF: time since fire (yr^{-1}).

Table 3: Model fitness to the data for *a priori* hypotheses for the FH horizon. Models are sorted by increasing second-order Akaike information criterion (AICc).

Hypothesis	Climate	Texture	C statistic	df	p	K	AIC_c	ΔAIC_c	W
FF2	**MAP**	**Clay %**	**22.30**	**26**	**0.67**	**11**	**48.77**	**0.00**	**0.68**
FF2	WB	Clay %	26.50	26	0.44	11	52.97	4.20	0.08
FF2	MAP	Sand %	27.28	26	0.39	11	53.76	4.99	0.06
FF2	MAP	Silt %	28.55	26	0.33	11	55.03	6.26	0.03

https://doi.org/10.5194/soil-2019-88
Preprint. Discussion started: 4 December 2019

FF2	WB	Sand %	28.93	26	0.31	11	55.41	6.64	0.02
FF2	MAT	Silt %	29.03	26	0.31	11	55.50	6.73	0.02
FF2	GDD5	Silt %	29.04	26	0.31	11	55.51	6.74	0.02
FF2	MAT	Clay %	29.29	26	0.30	11	55.76	6.99	0.02
FF2	MAT	Sand %	29.43	26	0.29	11	55.91	7.14	0.02
FF2	GDD5	Sand %	30.12	26	0.26	11	56.59	7.82	0.01
FF2	WB	Silt %	30.48	26	0.25	11	56.95	8.18	0.01
FF2	GDD5	Clay %	30.56	26	0.25	11	57.03	8.26	0.01
FF1	WB	Clay %	46.66	30	0.03	7	62.44	13.67	0.00
FF1	MAP	Clay %	47.95	30	0.02	7	63.73	14.96	0.00
FF1	WB	Sand %	50.53	30	0.01	7	66.30	17.53	0.00
FF1	WB	Silt %	53.50	30	0.01	7	69.27	20.50	0.00
FF1	MAP	Sand %	54.23	30	0.00	7	70.01	21.24	0.00
FF1	MAP	Silt %	56.92	30	0.00	7	72.70	23.93	0.00
FF1	GDD5	Clay %	57.79	30	0.00	7	73.57	24.80	0.00
FF1	GDD5	Sand %	58.62	30	0.00	7	74.40	25.63	0.00
FF1	GDD5	Silt %	58.89	30	0.00	7	74.67	25.90	0.00
FF1	MAT	Clay %	59.82	30	0.00	7	75.59	26.82	0.00
FF1	MAT	Sand %	61.19	30	0.00	7	76.97	28.20	0.00
FF1	MAT	Silt %	62.22	30	0.00	7	78.00	29.23	0.00

Note: *Hypothesis*: model name; *Climate*: climate variable; *Texture*: texture variable; *C statistic*: statistic for Fisher's *C* test; *df*: degree of freedom; *p*: p-value for Fisher's *C* test (when $p < 0.05$, the model is not supported by the data); *K*: number of free parameters; *AICc*: second order Akaike information criterion; Δ*AICc*: relative AICc difference with the model that best fitted the data (in bold); *W*: Akaike weight.

Table 4: Model fitness to the data for *a priori* hypotheses for the mineral soil. Models are sorted by increasing second-order Akaike information criterion (AICc).

Hypothesis	Climate	Texture	Exchangeable element	C statistic	df	p	K	AIC_c	ΔAIC_c	W
MIN2	**WB**	**Clay %**	**Al**	**27.76**	**24.00**	**0.27**	**14.00**	**63.26**	**0.00**	**0.47**
MIN2	MAP	Clay %	Al	30.18	24.00	0.18	14.00	65.68	2.42	0.14
MIN2	WB	Clay %	Mn	31.15	24.00	0.15	14.00	66.65	3.39	0.09
MIN2	GDD5	Clay %	Al	31.78	24.00	0.13	14.00	67.28	4.02	0.06
MIN2	MAT	Clay %	Al	32.21	24.00	0.12	14.00	67.71	4.45	0.05
MIN2	MAP	Clay %	Mn	32.81	24.00	0.11	14.00	68.31	5.05	0.04
MIN1	GDD5	Sand %	Mn	52.77	30.00	0.01	7.00	68.55	5.29	0.03
MIN2	GDD5	Clay %	Mn	34.34	24.00	0.08	14.00	69.84	6.58	0.02
MIN2	MAT	Clay %	Mn	34.57	24.00	0.08	14.00	70.07	6.81	0.02
MIN1	MAT	Sand %	Mn	54.44	30.00	0.00	7.00	70.22	6.96	0.01

https://doi.org/10.5194/soil-2019-88
Preprint. Discussion started: 4 December 2019

MIN1	GDD5	Clay %	Mn	54.78	30.00	0.00	7.00	70.55	7.29	0.01
MIN1	GDD5	Silt %	Mn	55.22	30.00	0.00	7.00	70.99	7.73	0.01
MIN2	GDD5	Sand %	Al	35.51	24.00	0.06	14.00	71.01	7.75	0.01
MIN1	MAT	Clay %	Mn	55.90	30.00	0.00	7.00	71.68	8.42	0.01
MIN2	GDD5	Sand %	Mn	36.21	24.00	0.05	14.00	71.71	8.45	0.01
MIN2	WB	Sand %	Al	36.26	24.00	0.05	14.00	71.76	8.50	0.01
MIN1	MAP	Clay %	Mn	56.70	30.00	0.00	7.00	72.48	9.22	0.00
MIN2	WB	Sand %	Mn	37.14	24.00	0.04	14.00	72.64	9.38	0.00
MIN1	WB	Clay %	Mn	57.54	30.00	0.00	7.00	73.31	10.05	0.00
MIN1	MAT	Silt %	Mn	57.65	30.00	0.00	7.00	73.43	10.17	0.00
MIN2	MAT	Sand %	Al	38.06	24.00	0.03	14.00	73.56	10.30	0.00
MIN2	GDD5	Silt %	Mn	38.19	24.00	0.03	14.00	73.69	10.43	0.00
MIN2	MAT	Sand %	Mn	38.44	24.00	0.03	14.00	73.93	10.67	0.00
MIN1	WB	Sand %	Mn	58.57	30.00	0.00	7.00	74.34	11.08	0.00
MIN2	GDD5	Silt %	Al	39.04	24.00	0.03	14.00	74.53	11.27	0.00
MIN1	MAP	Sand %	Mn	60.15	30.00	0.00	7.00	75.92	12.66	0.00
MIN2	MAT	Silt %	Mn	41.32	24.00	0.02	14.00	76.82	13.56	0.00
MIN2	MAP	Sand %	Al	41.49	24.00	0.01	14.00	76.99	13.73	0.00
MIN2	MAP	Sand %	Mn	41.88	24.00	0.01	14.00	77.38	14.12	0.00
MIN2	MAT	Silt %	Al	42.64	24.00	0.01	14.00	78.14	14.88	0.00
MIN2	WB	Silt %	Mn	42.64	24.00	0.01	14.00	78.14	14.88	0.00
MIN2	WB	Silt %	Al	43.25	24.00	0.01	14.00	78.75	15.49	0.00
MIN1	WB	Silt %	Mn	63.72	30.00	0.00	7.00	79.49	16.23	0.00
MIN1	MAP	Silt %	Mn	65.01	30.00	0.00	7.00	80.79	17.53	0.00
MIN2	MAP	Silt %	Mn	47.03	24.00	0.00	14.00	82.53	19.27	0.00
MIN1	GDD5	Sand %	Al	67.22	30.00	0.00	7.00	83.00	19.74	0.00
MIN2	MAP	Silt %	Al	47.77	24.00	0.00	14.00	83.27	20.01	0.00
MIN1	MAT	Sand %	Al	68.01	30.00	0.00	7.00	83.79	20.53	0.00
MIN1	WB	Sand %	Al	69.72	30.00	0.00	7.00	85.50	22.24	0.00
MIN1	MAP	Sand %	Al	72.48	30.00	0.00	7.00	88.26	25.00	0.00
MIN1	GDD5	Silt %	Al	72.85	30.00	0.00	7.00	88.63	25.37	0.00
MIN1	MAT	Silt %	Al	74.41	30.00	0.00	7.00	90.19	26.93	0.00
MIN1	WB	Clay %	Al	74.57	30.00	0.00	7.00	90.35	27.09	0.00
MIN1	MAP	Clay %	Al	74.92	30.00	0.00	7.00	90.69	27.43	0.00
MIN1	GDD5	Clay %	Al	75.10	30.00	0.00	7.00	90.88	27.62	0.00
MIN1	MAT	Clay %	Al	75.36	30.00	0.00	7.00	91.13	27.87	0.00
MIN1	WB	Silt %	Al	78.06	30.00	0.00	7.00	93.83	30.57	0.00

https://doi.org/10.5194/soil-2019-88
Preprint. Discussion started: 4 December 2019

MIN1	MAP	Silt %	Al		80.53	30.00	0.00	7.00	96.31	33.05	0.00

Note: *Hypothesis*: model name; *Climate*: climate variable; *Texture*: texture variable; *Exchangeable element*: exchangeable element variable; *C statistic*: statistic for Fisher's *C* test; *df*: degree of freedom; *p*: p-value for Fisher's *C* test (when $p < 0.05$, the model is not supported by the data); *K*: number of free parameters; *AICc*: second order Akaike information criterion; Δ*AICc*: relative AICc difference with the model that best fitted the data (in bold); *W*: Akaike weight.

735

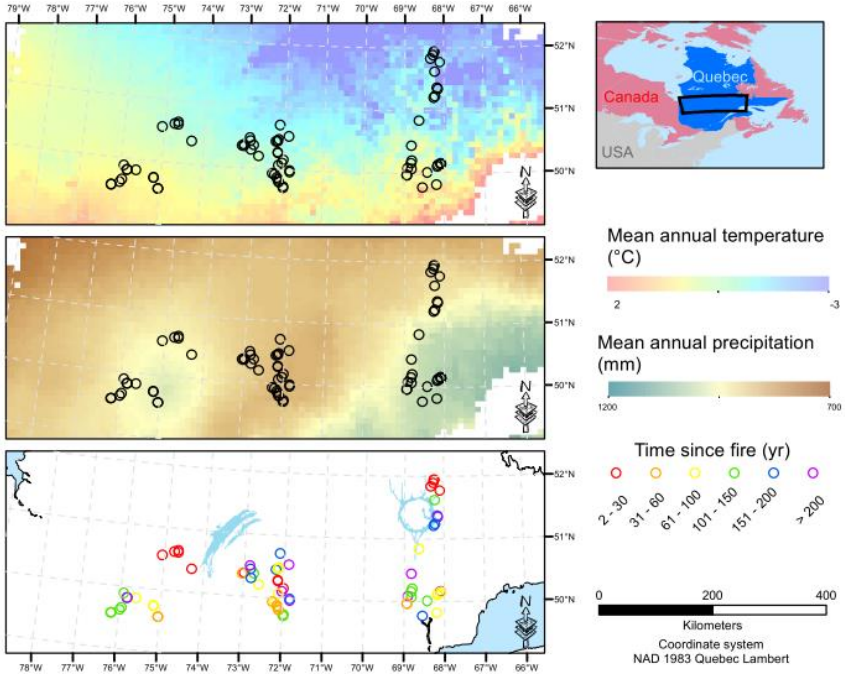

Figure 1: Map of the study area showing the location of the sample plots. Mean annual temperature (upper panel) and mean annual precipitation (middle panel) are interpolations from the 1981–2010 Canadian climate normals on a 10 x 10 km pixel grid (Chaste et al. 2018). The lower panel presents the location of the sample plots in relation to time since fire (yr^{-1}).

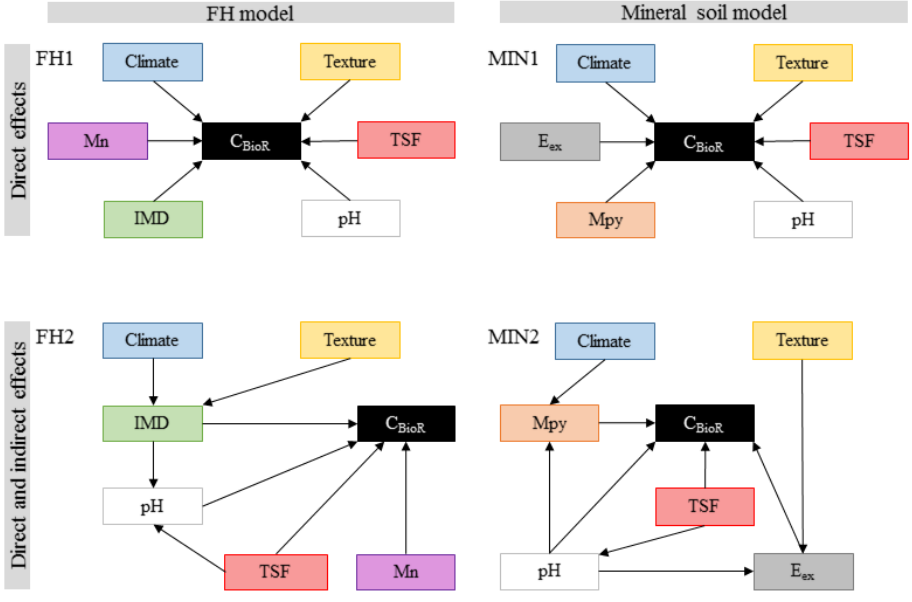

740

https://doi.org/10.5194/soil-2019-88
Preprint. Discussion started: 4 December 2019

Figure 2: Path models for each of the multivariate causal hypotheses. Arrows indicate direct causal relationships. *Climate*: climate variable; *Texture*: texture variable; *TSF*: time since fire; *pH*: pH of the FH horizon (FH1 and FH2) or of the top 35 cm of mineral soil (MIN1 and MIN2); *IMD*: index of moss dominance; *Mn*: exchangeable manganese of the FH horizon; *Mpy*: pyrophosphate extractable metals; E_{ex}: exchangeable element (Al or Mn) of the mineral soil.

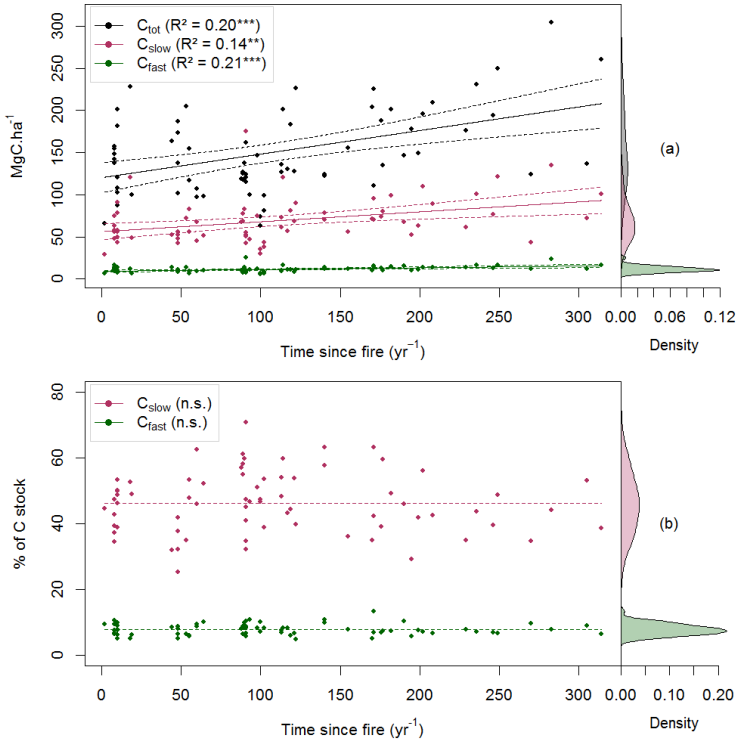

Figure 3: Carbon quality as a function of time since fire (TSF). The upper panel shows the total soil C reservoir (C_{tot}), the recalcitrant C pool (C_{slow}) and the bioreactive C pool (C_{fast}) sizes as a function of TSF (a, on the left), and the kernel density for each pool (a, on the right). The lower panel shows the proportion of C_{slow} and C_{fast} relative to C_{tot} as a function of TSF (b, on the left), and their kernel density (b, on the right).

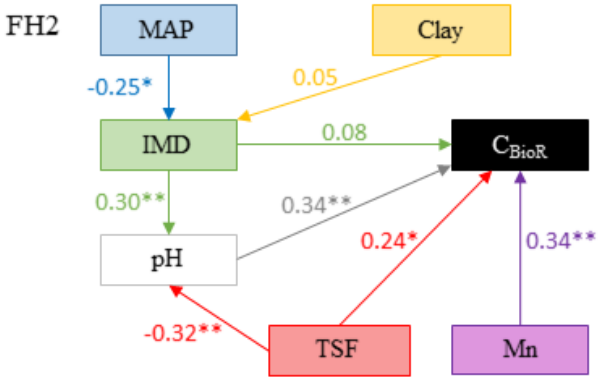

Figure 4: Model that best fitted the data to explain carbon bioreactivity (C_{BioR}) in the FH horizon. Arrows indicate direct causal relationships. The numbers are standardized averaged path coefficients obtained using model averaging (see Table S1 and text

https://doi.org/10.5194/soil-2019-88
Preprint. Discussion started: 4 December 2019

for further details). *MAP*: mean annual precipitation; *Clay*: clay content in the top 35 cm of mineral soil; *Mn*: exchangeable manganese; *pH*: pH of the FH horizon; *TSF*: time since fire; *IMD*: index of moss dominance. (*) $p < 0.05$; (**) $p < 0.01$.

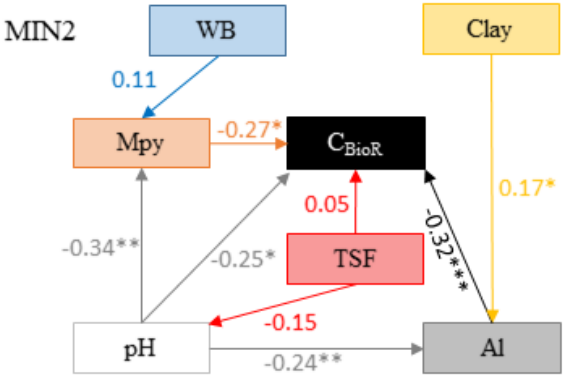

Figure 5: Model that best fitted the data to explain the carbon bioreactivity (C_{BioR}) in the top 35 cm of the mineral soil. Arrows indicate direct causal relationships. The numbers are standardized averaged path coefficients obtained using model averaging (see Table S2 and text for further details). *Al*: exchangeable aluminum in the top 35 cm of the mineral soil; *pH*: pH of the top 35 cm of the mineral soil; *TSF*: time since fire; *Mpy*: metal oxide content in the top 15 cm of the B horizon; *WB*: water balance; *Clay*: clay content of the top 35 cm of the mineral soil. (*) $p < 0.05$; (**) $p < 0.01$; (***) $p < 0.001$.